Available online at www.sciencedirect.com

ScienceDirect

International Journal of Thermal Sciences 47 (2008) 1701–1711

International Journal of Thermal Sciences

www.elsevier.com/locate/ijts

Entropy analysis for non-linear viscoelastic fluid in concentric rotating cylinders

M. Mirzazadeh, A. Shafaei, F. Rashidi *

Department of Chemical Engineering, Amirkabir University of Technology, Hafez Ave., No. 424, Tehran, Iran

Received 11 June 2006; received in revised form 26 October 2007; accepted 13 November 2007

Available online 20 June 2008

Abstract

An analytical solution is presented for the forced convection and entropy generation of a viscoelastic fluid obeying the Phan-Thien–Tanner (PTT) constitutive equation in a concentric annulus with relative rotation of the inner and outer cylinders. Two different types of boundary conditions are considered: at the first case both cylinders are isothermal and kept at different temperatures and in the second case the heat flux is kept constant at the outer cylinder and the inner one is isothermal. Analytical expressions for dimensionless temperature profile (Θ), dimensionless entropy generation number (N_S), and the Bejan number (Be) are obtained. The effect of velocity ratio (β), the group parameter (Br/Ω), the Brinkman number (Br), and fluid elasticity (εWe^2) on the above parameters are investigated. The results show that the total entropy generation number decreases as the fluid elasticity increases. The results also show that entropy generation number increases with increasing Brinkman number.

Keywords: Entropy generation; Annular flow; Phan-Thien–Tanner constitutive equation; Analytical solution; Heat transfer

1. Introduction

Tangential flows of non-Newtonian fluids within annuli have wide range of engineering applications such as in the journal bearings, commercial viscometers, swirl nozzles, chemical and mechanical mixing equipments and electrical motors (see e.g. Maron and Cohen [1]).

Forced convective heat transfer of Newtonian fluids in annular space has been investigated extensively in the literature. A comprehensive review of paper is given by Childs and Long [2].

An extensive bibliography of papers on the flow of non-Newtonian fluids through annular channels is given in a recent paper by Escudier et al. [3]. Convective heat transfer of non-Newtonian fluids inside the annuli were considered in several works, for example Khellaf and Lauriat [4] analyzed the convective heat transfer characteristics for the flow of a Carreau fluid between rotating concentric vertical cylinders. Naimi et al. [5] performed a flow visualization study of the development and structure of Taylor–Couette vortices for the case of a power-law fluid (Carbopol 940) with and without axial flow in the forced convection regime. From their experimental study, they derived heat transfer correlations for various flow regimes. Laminar forced convection heat transfer of purely viscous, non-Newtonian fluid flow in both concentric and eccentric annuli was numerically investigated by Manglik and Fang [6]. Capobianchi and Irvine [7] have considered heat transfer to modified power-law liquids in concentric annuli.

Although the forgoing research works have covered a wide range of problems involving the flow and heat transfer in concentric annuli they have been restricted, from thermodynamic point of view, to only the first law (thermodynamic) analysis. The contemporary trend in the field of heat transfer and thermal design is the second law (of thermodynamics) analysis and its design-related concept of entropy generation minimization (Bejan [8]). Entropy generation is associated with thermodynamic irreversibility, which is common in all types of heat transfer processes. The ultimate motive behind the infusion of entropy generation analysis in heat transfer and thermal design is economics, and it is clear that minimizing irreversibility in the thermal systems results in decreasing the operating cost. Since

* Corresponding author. Tel.: +9821 6499066; fax: +9821 6405847.
E-mail addresses: mirzazadeh_m@yahoo.com (M. Mirzazadeh), shafaei_a@cic.aut.ac.ir (A. Shafaei), rashidi@aut.ac.ir (F. Rashidi).

1290-0729/$ – see front matter
doi:10.1016/j.ijthermalsci.2007.11.002

Nomenclature

Be	Bejan number, $= N_R/N_S$	
Br	Brinkman number, $= Ec \times Pr$	
C	constant (see Eq. (39))	
C_n	integration constants, $n = 2, 3, 4$	
C_P	specific heat at constant pressure	$\mathrm{kJ\,kg^{-1}\,K^{-1}}$
E	constant (see Eq. (39))	
Ec	Eckert number, $= (r_i\omega_i)^2/(C_P\Delta T)$	
F	constant (see Eq. (39))	
k	thermal conductivity	$\mathrm{W\,m^{-1}\,K^{-1}}$
N_F	entropy generation number; fluid friction contribution	
N_R	entropy generation number; heat transfer contribution	
N_S	entropy generation number; total	
$\tilde{p}$	constant (see Eq. (12))	
Pr	Prandtl number, $= \eta C_P/k$	
$\tilde{q}$	constant (see Eq. (13))	
q	constant heat flux at wall	$\mathrm{W\,m^{-2}}$
r	radial distance	m
R	dimensionless radial distance, $= r/r_i$	
S_G	entropy generation rate	$\mathrm{W\,m^{-3}\,K^{-1}}$
T	temperature	°C
u	tangential velocity	$\mathrm{m\,s^{-1}}$
U	dimensionless tangential velocity, $= u/u_c$	
u_c	characteristic velocity, $= r_i\omega_i$	
We	Weissenberg number, $= \lambda u_c/\delta$	
Z	stress coefficient function (see Eq. (7))	

Greek symbols

α	thermal diffusivity	$\mathrm{m^2\,s^{-1}}$
β	velocity ratio, $= (r_o\omega_o)/(r_i\omega_i)$	
δ	annular gap, $r_o - r_i$	m
ε	elongational parameter of the PTT model	
η	viscosity coefficient of the PTT model	Pa s
$\dot{\gamma}$	shear rate tensor	$\mathrm{s^{-1}}$
λ	relaxation time in PTT model	s
ω	angular velocity	$\mathrm{rad\,s^{-1}}$
Ω	dimensionless temperature difference, $= \Delta T/T_i$	
Φ	viscous dissipation function (see Eq. (23))	
Π	radius ratio, $= r_o/r_i$	
τ	stress tensor	Pa
θ	tangential coordinate	
Θ	dimensionless temperature, $= (T - T_i)/\Delta T$	
$\forall$	volume of the annular gap	$\mathrm{m^3}$

Superscripts

T	transpose of tensor
$*$	refers to dimensionless quantities

Subscripts

av	refers to average value
i	refers to inner cylinder
o	refers to outer cylinder
q	refers to isoflux boundary condition
T	refers to isothermal boundary condition
w	refers to wall value

the lost available work is proportional to the entropy generation, thus decreasing entropy generation decreases the lost available work. Different sources are responsible for the generation of entropy (Bejan [8]), for example, heat transfer across a finite temperature difference, characteristics of convective heat transfer, viscous effects, etc.

The concepts of entropy generation number and irreversibility distribution ratio were introduced by Bejan [9], a considerable number of research studies were carried out to examine entropy generation in the flow systems with different geometric configurations, flow situations, and thermal boundary conditions. Bejan [9] obtained the entropy generation in fundamental convective heat transfer problems and provided some examples. Nag and Kumar [10] presented the second law optimization techniques for convective heat transfer through duct at constant heat flux boundary condition. Further extension was done by Sahin [11] who introduced the second law analysis of viscous fluid in a circular duct at isothermal boundary condition. In a more recent paper, Sahin [12] presented the effect of variable viscosity on entropy generation rate for the constant heat flux boundary condition for circular ducts.

For a concentric cylindrical annulus, Yilbas [13] presented an entropy analysis with a rotating outer cylinder and differentially heated isothermal boundary condition. Yilbas assumed a linear velocity profile and neglected the contribution of fluid friction irreversibility to entropy generation. Analysis of entropy generation inside concentric cylindrical annuli with relative rotation was investigated by Mahmud and Fraser [14]. They showed that irreversibility increased with increasing Brinkman number and group parameters, except when both cylinders rotate in the same direction with the same angular speed. Haddad et al. [15] focused on entropy generation due to the laminar forced convection in the entrance region of a concentric cylindrical annulus. They found that entropy generation is inversely proportional to both Reynolds number and the dimensionless entrance temperature.

Second law analysis of channel and pipe flows for non-Newtonian power-law fluids was carried out by Mahmud and Fraser [16]. Pakdemirli and Yilbas [17] presented the entropy generation for pipe flow of a third grade fluid with Vogel model viscosity.

Although many studies on the energy and exergy analysis of thermal systems and their applications have recently been undertaken by some researchers, to the best knowledge of the authors, entropy generation analysis for viscoelastic fluid has not yet been addressed in the literature and the present study is considered as a first attempt in this context.

The Phan-Thien–Tanner (PTT) model is a fairly simple quasi-linear viscoelastic model constitutive equation which was derived using network theory by Phan-Thien and Tanner [18] and Phan-Thien [19]. This model incorporates not only shear-thinning shear viscosity, normal-stress differences but also an elongational parameter ε and so reproduces many of the characteristics of the rheology of polymer solutions and other liquids. The elongational parameter imposes an upper limit on the elongational viscosity which is inversely proportional to ε. When ε goes to zero the PTT constitutive equation reduces to the Johnson–Segalman model but without the presence of the solvent viscosity, while the simplified form of the PTT model is equivalent to the upper convected Maxwell model. The PTT model is being employed increasingly to predict the flow and heat transfer of viscoelastic fluids: Recent papers include those of Oliveira and Pinho [20], Cruz and Pinho [21] and Mirzazadeh et al. [22].

The objective of present paper is to determine heat transfer characteristics and the resulting entropy generation in purely tangential flow of nonlinear viscoelastic fluid obeying simplified form of Phan-Thien–Tanner (SPTT) constitutive equation between concentric rotating cylinders where the inner and the outer cylinders are rotating with different angular velocities. The governing equations are simplified and solved using both isothermal and isoflux boundary conditions. Analytical expressions for dimensionless entropy generation number, irreversibility distribution ratio, and the Bejan number are obtained.

2. Mathematical formulation

Fig. 1 presents a schematic diagram of the fluid flow and heat transfer domains. The ratio of outer cylinder radius (r_o) to inner cylinder radius (r_i) is defined as Π, so that the radial gap width, δ is equal to $(\Pi - 1)r_i$. The angular velocities of the inner and outer cylinders are denoted by ω_i and ω_o, respectively.

The problem under consideration is steady, laminar, and purely tangential, therefore the radial component of velocity vector is neglected. Also the fluid properties are assumed to be independent of temperature. Under these conditions, the governing energy equation describing this problem, with the assumption of appreciable viscous dissipation and negligible axial flow, can be represented by the following equation:

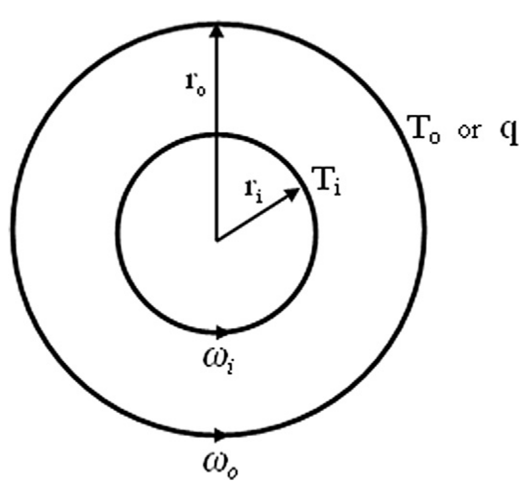

Fig. 1. Schematic view of concentric rotating annuli.

$$\frac{k}{r}\frac{\mathrm{d}}{\mathrm{d}r}\left(r\frac{\mathrm{d}T}{\mathrm{d}r}\right) + \tau_{r\theta} r \frac{\mathrm{d}}{\mathrm{d}r}\left(\frac{u_\theta}{r}\right) = 0 \tag{1}$$

In this study, two types of boundary conditions are considered: in the first case, both cylinders are isothermal and kept at different temperatures and in the second case, the inner cylinder is subjected to a constant temperature while the outer cylinder is kept at constant heat flux. The boundary conditions are:

$$r = r_i \quad \Rightarrow \quad u_\theta = r_i\omega_i,\ T = T_i \tag{2}$$

$$r = r_o \quad \Rightarrow \quad u_\theta = r_o\omega_o,\ T = T_o \text{ or } \frac{\partial T}{\partial r} = \frac{q}{k} \tag{3}$$

Let us introduce a characteristic velocity scale $u_c = r_i\omega_i$ together with the Brinkman number ($Br = Ec \times Pr$, where Ec is the Eckert number and Pr is the Prandtl number) and a characteristic shear stress ($\eta u_c/\delta$). Following the introduction of these parameters, Eq. (1) can be written in non-dimensional form as:

$$\frac{1}{R}\frac{\mathrm{d}}{\mathrm{d}R}\left(R\frac{\mathrm{d}\Theta}{\mathrm{d}R}\right) + \frac{Br}{\Pi - 1}\tau^*_{r\theta} R \frac{\mathrm{d}}{\mathrm{d}R}\left(\frac{U}{R}\right) = 0 \tag{4}$$

where $R = r/r_i$, and Θ is the dimensionless temperature and is defined as $(T - T_i)/\Delta T$ (where $\Delta T = T_o - T_i$ is the reference temperature difference), $\tau^*_{r\theta}$ is dimensionless shear stress and is defined as $\tau_{r\theta}/(\eta u_c/\delta)$, and U is dimensionless velocity (u_θ/u_c).

3. Analytical solution

3.1. Fluid constitutive equation

In this investigation the simplified Phan-Thien–Tanner (SPTT) constitutive equation with linearized stress coefficient was employed. This rheological equation (SPTT) can be described by the following expression (Phan-Thien and Tanner [18] and Phan-Thien [19]):

$$Z(\operatorname{tr}\tau)\tau + \lambda\tau_{(1)} = \eta\dot{\gamma} \tag{5}$$

where η is the viscosity coefficient of the model, λ is the relaxation time, $\operatorname{tr}\tau$ is the trace of the stress tensor and $\tau_{(1)}$ is the upper convected time derivative of the stress tensor:

$$\tau_{(1)} = \frac{\mathrm{D}\tau}{\mathrm{D}t} - \left\{(\nabla V)^T.\tau + \tau.(\nabla V)\right\} \tag{6}$$

The stress coefficient Z has an exponential form but can be linearized when the deformation rate of fluid element is small; a condition which corresponds to what Tanner [23] classifies as weak flow:

$$Z(\operatorname{tr}\tau) = 1 + \frac{\varepsilon\lambda}{\eta}\operatorname{tr}\tau \tag{7}$$

where ε is the elongational parameter of the model.

3.2. Hydrodynamic solution

The hydrodynamic solution for the tangential flow of SPTT was derived by Mirzazadeh et al. [22] who arrived at the following equations for dimensionless velocity profile, shear rate, and shear stress:

$$\frac{U}{R} = -\frac{\tau_{wi}^*}{(\Pi-1)R^2}\left[\frac{1}{2} + \frac{\varepsilon We^2 \tau_{wi}^{*2}}{3R^4}\right] + C_2 \tag{8}$$

$$\dot{\gamma}^* = (\Pi-1)R\frac{\mathrm{d}}{\mathrm{d}R}\left(\frac{U}{R}\right) = \tau_{r\theta}^*\left(1 + 2\varepsilon We^2 \tau_{r\theta}^{*2}\right) \tag{9}$$

$$\tau_{r\theta}^* = \frac{\tau_{wi}^*}{R^2} \tag{10}$$

where We is Weissenberg number, a measure of the level of elasticity in the fluid (defined as, $We = \lambda u_c/\delta$) and τ_{wi}^* is the dimensionless wall shear stress on the inner cylinder and was shown to be given by:

$$\tau_{wi}^* = \frac{1}{6}\sqrt[3]{-108\tilde{q} + 12\sqrt{12\tilde{p}^3 + 81\tilde{q}^2}} - \frac{2\tilde{p}}{\sqrt[3]{-108\tilde{q} + 12\sqrt{12\tilde{p}^3 + 81\tilde{q}^2}}} \tag{11}$$

The constants $\tilde{p}$ and $\tilde{q}$ in Eq. (11) are given by:

$$\tilde{p} = \frac{3\Pi^4(\Pi^2-1)}{2\varepsilon We^2(\Pi^6-1)} \tag{12}$$

$$\tilde{q} = \frac{3\Pi^5(\Pi-1)(\Pi-\beta)}{\varepsilon We^2(\Pi^6-1)} \tag{13}$$

where

$$\beta = \frac{r_o\omega_o}{r_i\omega_i} \tag{14}$$

Once τ_{wi}^* is known, determination of constant C_2 in Eq. (8) is straightforward: C_2 is obtained from Eq. (8) and by applying one of the boundary conditions (Eq. (2) or Eq. (3)).

For the limiting case ($\varepsilon We^2 \to 0$) Eq. (8) reduces to the well-known solution for a Newtonian fluid (see e.g. Bird et al. [24]; Mahmud and Fraser [14])

$$\frac{U}{R} = -\frac{\tau_{wi}^*}{2(\Pi-1)R^2} + C_2 \tag{15}$$

where

$$\tau_{wi}^* = -\frac{2\Pi(\Pi-\beta)}{\Pi+1} \quad \text{and} \quad C_2 = \frac{\beta\Pi-1}{\Pi^2-1} \tag{16}$$

3.3. First law analysis

Substitution Eqs. (9) and (10) into Eq. (4) and integrating, the dimensionless temperature profile can be obtained:

$$\Theta = -\frac{Br\,\tau_{wi}^{*2}}{4R^2(\Pi-1)^2} - \frac{\varepsilon We^2 Br\,\tau_{wi}^{*4}}{18R^6(\Pi-1)^2} + C_3\ln R + C_4 \tag{17}$$

In the above equation, C_3 and C_4 are the constants of integration which can be obtained by introduction of boundary conditions into temperature profile. For the isothermal boundary condition, $\Theta = 0$ at $R = 1$ and $\Theta = 1$ at $R = \Pi$. Using these dimensionless boundary conditions, non-dimensional temperature profile for the isothermal boundary condition becomes

$$\begin{aligned}\Theta_T = {} & \frac{Br\,\tau_{wi}^{*2}}{36R^6(\Pi-1)^2}\left[9R^4(R^2-1) + 2\varepsilon We^2\tau_{wi}^{*2}(R^6-1)\right] \\ & + \left[1 + \frac{Br\,\tau_{wi}^{*2}}{36\Pi^6(\Pi-1)^2}\left(9\Pi^4(1-\Pi^2)\right.\right. \\ & \left.\left. + 2\varepsilon We^2\tau_{wi}^{*2}(1-\Pi^6)\right)\right]\frac{\ln R}{\ln \Pi}\end{aligned} \tag{18}$$

For the limiting case of Newtonian fluid (as εWe^2 goes to zero) the previous equation reduces to the following expression for temperature profile:

$$\Theta_T = Br\left(\frac{\Pi(\Pi-\beta)}{\Pi^2-1}\right)^2\left[1 - \frac{1}{R^2} + \left(\frac{1}{\Pi^2} - 1\right)\frac{\ln R}{\ln \Pi}\right] + \frac{\ln R}{\ln \Pi} \tag{19}$$

As it can be seen from the above equation, our result is not in agreement with the previous work of Mahmud and Fraser [14] (compare Eq. (9) in their work with Eq. (19) in our). We believe that, the reason of this discrepancy is related to the mistake occurred at the early stages of their analysis which had a 'knock-on' effect throughout their paper.

For the isoflux boundary condition, a constant heat flux q is applied to the outer cylinder, but the temperature at the inner cylinder is kept constant as isothermal case. For this particular case, $\Theta = 0$ at $R = 1$ and $\partial\Theta/\partial R = 1$ at $R = \Pi$. Using these dimensionless boundary conditions, non-dimensional temperature distribution for the isoflux boundary condition becomes

$$\begin{aligned}\Theta_q = {} & \frac{Br\,\tau_{wi}^{*2}}{36R^6(\Pi-1)^2}\left[9R^4(R^2-1) + 2\varepsilon We^2\tau_{wi}^{*2}(R^6-1)\right] \\ & + \left[1 - \frac{Br\,\tau_{wi}^{*2}}{6\Pi^7(\Pi-1)^2}\left(3\Pi^4 + 2\varepsilon We^2\tau_{wi}^{*2}\right)\right]\Pi\ln R\end{aligned} \tag{20}$$

For the limiting case of Newtonian fluid (as εWe^2 goes to zero) the previous equation reduces to the following expression for temperature profile:

$$\Theta_q = Br\left(\frac{\Pi(\Pi-\beta)}{\Pi^2-1}\right)^2\left(1 - \frac{1}{R^2} - \frac{2\ln R}{\Pi^2}\right) + \Pi\ln R \tag{21}$$

As it can be seen from the above equation, our result is basically similar in shape to that of Mahmud and Fraser [14] (see Eq. (10) in their work), but again there is a small difference; the constant Γ_3 in their work ($\frac{(\Pi-\beta)^2}{\Pi^2-1}$, see paragraph below Eq. (8) in [14]) is not equal to $(\frac{\Pi(\Pi-\beta)}{\Pi^2-1})^2$ of this work, as it can be seen on the right-hand side of Eq. (21).

3.4. Second law analysis

The local volumetric rate of entropy generation, S_G ($\mathrm{W\,m^{-3}\,K^{-1}}$), in cylindrical coordinates is given in the following equation (Bejan [25])

$$S_G = \frac{\kappa}{T_i^2}(\nabla T)^2 + \frac{\Phi}{T_i} \tag{22}$$

Function Φ appearing in Eq. (22) is the viscous dissipation function and can be obtained from the following equation:

$$\Phi = \tau_{r\theta} r \frac{\mathrm{d}}{\mathrm{d}r}\left(\frac{u_\theta}{r}\right) \tag{23}$$

Substitution Eq. (23) into Eq. (22) leads to

$$S_G = \frac{k}{T_i^2}\left(\frac{\mathrm{d}T}{\mathrm{d}r}\right)^2 + \frac{\tau_{r\theta}}{T_i} r \frac{\mathrm{d}}{\mathrm{d}r}\left(\frac{u_\theta}{r}\right) \tag{24}$$

Eq. (24) clearly shows contributions of the two sources of entropy generations. The first term on the right-hand side of Eq. (24) is the entropy generation due to heat transfer across a finite temperature difference, whereas the second term is the local entropy generation due to viscous dissipation. It is also appropriate to define dimensionless group for entropy generation rate, as the entropy generation number (N_S). This new group is defined by dividing the volumetric entropy generation rate (S_G) to a characteristic entropy generation rate ($S_{G,C}$). For two cases of isoflux and isothermal boundary conditions the characteristic entropy generation rates are as below (Bejan [8,9]):

$$S_{G,C} = \left[\frac{q^2}{\kappa T_i^2}\right]_{\text{Isoflux}}, \qquad S_{G,C} = \left[\frac{\kappa(\Delta T)^2}{r_i^2 T_i^2}\right]_{\text{Isothermal}} \tag{25}$$

Using the above characteristic entropy generation rates and with respect to definition of entropy generation number, we arrive at the following equation for N_S

$$N_S = \left(\frac{\mathrm{d}\Theta}{\mathrm{d}R}\right)^2 + \frac{Br\,\tau_{r\theta}^*}{\Omega(\Pi - 1)} R \frac{\mathrm{d}}{\mathrm{d}R}\left(\frac{U}{R}\right) = N_R + N_F \tag{26}$$

where Ω is the dimensionless temperature difference ($\Delta T/T_i$). The first term on the right-hand side of Eq. (26), is entropy generation due to heat transfer in radial direction (N_R) and the second term is the fluid friction contribution to entropy generation (N_F). Substitution Eqs. (9) and (18) into Eq. (26), gives the entropy generation number (N_{ST}) for the case of isothermal boundary condition

$$\begin{aligned} N_{ST} = {} & \left\{ \frac{Br\,\tau_{wi}^{*2}}{6(\Pi-1)^2 R^7}\left(3R^4 + 2\varepsilon\, We^2\, \tau_{wi}^{*2}\right) \right. \\ & + \left[1 + \frac{Br\,\tau_{wi}^{*2}}{36(\Pi-1)^2\Pi^6}\left(9\Pi^4\left(1-\Pi^2\right) \right.\right. \\ & \left.\left.\left. + 2\varepsilon\, We^2\, \tau_{wi}^{*2}\left(1-\Pi^6\right)\right)\right] \Big/ R\ln\Pi \right\}^2 \\ & + \frac{Br}{\Omega}\frac{\tau_{wi}^{*2}}{(\Pi-1)^2 R^8}\left(R^4 + 2\varepsilon\, We^2\, \tau_{wi}^{*2}\right) \end{aligned} \tag{27}$$

Substitution Eqs. (9) and (19) into Eq. (26) gives the entropy generation number (N_{Sq}) for the case of isoflux boundary condition

$$\begin{aligned} N_{Sq} = {} & \left\{ \frac{Br\,\tau_{wi}^{*2}}{6(\Pi-1)^2 R^7}\left(3R^4 + 2\varepsilon\, We^2\, \tau_{wi}^{*2}\right) \right. \\ & \left. + \left[1 - \frac{Br\,\tau_{wi}^{*2}}{6(\Pi-1)^2\Pi^7}\left(3\Pi^4 + 2\varepsilon\, We^2\, \tau_{wi}^{*2}\right)\right]\frac{\Pi}{R} \right\}^2 \\ & + \frac{Br\,\tau_{wi}^{*2}}{\Omega(\Pi-1)^2 R^8}\left(R^4 + 2\varepsilon\, We^2\, \tau_{wi}^{*2}\right) \end{aligned} \tag{28}$$

Br/Ω in Eqs. (27) and (28) determines the relative importance between viscous effects and fluid conduction effects. Because flow and thermal fields are assumed independent, it can be easily seen from Eqs. (27) and (28) that, the fluid friction contribution to the entropy generation are the same, for both isothermal and isoflux boundary conditions.

For the limiting case of Newtonian fluid (as $\varepsilon\, We^2$ goes to zero) Eqs. (27) and (28) reduce to the following expressions for entropy generation number:

$$\begin{aligned} N_{ST} = {} & \left\{ Br\left(\frac{\Pi(\Pi-\beta)}{\Pi^2-1}\right)^2\left(\frac{2}{R^3} + \frac{1-\Pi^2}{\Pi^2}\frac{1}{R\ln\Pi}\right) \right. \\ & \left. + \frac{1}{R\ln\Pi} \right\}^2 + 4\frac{Br}{\Omega}\left(\frac{\Pi(\Pi-\beta)}{\Pi^2-1}\right)^2\frac{1}{R^4} \end{aligned} \tag{29}$$

$$\begin{aligned} N_{Sq} = {} & \left\{ 2\left(\frac{\Pi(\Pi-\beta)}{\Pi^2-1}\right)^2\frac{Br}{R}\left(\frac{1}{R^2} - \frac{1}{\Pi^2}\right) + \frac{\Pi}{R} \right\}^2 \\ & + 4\frac{Br}{\Omega}\left(\frac{\Pi(\Pi-\beta)}{\Pi^2-1}\right)^2\frac{1}{R^4} \end{aligned} \tag{30}$$

which again are not in agreement to those of Mahmud and Fraser [14] (compare Eqs. (14) and (15) of their work with Eqs. (29) and (30)).

3.5. *Fluid friction versus heat transfer irreversibility*

An important parameter in entropy generation analysis is the Bejan number, Be, which is the ratio of entropy generation due to heat transfer to the total entropy generation. The Bejan number defined by Paoletti et al. [26] is as below

$$Be = \frac{N_R}{N_R + N_F} \tag{31}$$

The Bejan number varies between 0 and 1. Accordingly, $Be = 1$ corresponds to the condition at which the entropy generation is dominated by heat transfer, while $Be = 0$ corresponds to the condition at which the fluid friction dominates the entropy generation. The Bejan number for the case of isothermal boundary condition can be obtained by using Eqs. (27) and (31)

$$\begin{aligned} Be_T = {} & \left\{ \frac{Br\,\tau_{wi}^{*2}}{6(\Pi-1)^2 R^7}\left(3R^4 + 2\varepsilon\, We^2\, \tau_{wi}^{*2}\right) \right. \\ & + \left[1 + \frac{Br\,\tau_{wi}^{*2}}{36(\Pi-1)^2\Pi^6}\left(9\Pi^4\left(1-\Pi^2\right) \right.\right. \\ & \left.\left.\left. + 2\varepsilon\, We^2\, \tau_{wi}^{*2}\left(1-\Pi^6\right)\right)\right] \Big/ R\ln\Pi \right\}^2 \\ & \times \left(\left\{ \frac{Br\,\tau_{wi}^{*2}}{6(\Pi-1)^2 R^7}\left(3R^4 + 2\varepsilon\, We^2\, \tau_{wi}^{*2}\right) \right.\right. \\ & + \left[1 + \frac{Br\,\tau_{wi}^{*2}}{36(\Pi-1)^2\Pi^6}\left(9\Pi^4\left(1-\Pi^2\right) \right.\right. \\ & \left.\left.\left. + 2\varepsilon\, We^2\, \tau_{wi}^{*2}\left(1-\Pi^6\right)\right)\right] \Big/ R\ln\Pi \right\}^2 \\ & \left. + \frac{Br\,\tau_{wi}^{*2}}{\Omega(\Pi-1)^2 R^8}\left(R^4 + 2\varepsilon\, We^2\, \tau_{wi}^{*2}\right)\right)^{-1} \end{aligned} \tag{32}$$

By combination of Eqs. (28) and (31) we arrive at the following expression for Bejan number for isoflux boundary condition

$$\begin{aligned} Be_q = {} & \left\{ \frac{Br\,\tau_{wi}^{*2}}{6(\Pi-1)^2 R^7}\left(3R^4 + 2\varepsilon\, We^2\, \tau_{wi}^{*2}\right) \right. \\ & \left. + \left[1 - \frac{Br\,\tau_{wi}^{*2}}{6(\Pi-1)^2 \Pi^7}\left(3\Pi^4 + 2\varepsilon\, We^2\, \tau_{wi}^{*2}\right)\right]\frac{\Pi}{R} \right\}^2 \\ & \times \left(\left\{ \frac{Br\,\tau_{wi}^{*2}}{6(\Pi-1)^2 R^7}\left(3R^4 + 2\varepsilon\, We^2\, \tau_{wi}^{*2}\right) \right. \right. \\ & \left. + \left[1 - \frac{Br\,\tau_{wi}^{*2}}{6(\Pi-1)^2 \Pi^7}\left(3\Pi^4 + 2\varepsilon\, We^2\, \tau_{wi}^{*2}\right)\right]\frac{\Pi}{R} \right\}^2 \\ & \left. + \frac{Br\,\tau_{wi}^{*2}}{\Omega(\Pi-1)^2 R^8}\left(R^4 + 2\varepsilon\, We^2\, \tau_{wi}^{*2}\right) \right)^{-1} \end{aligned} \tag{33}$$

For the limiting case of Newtonian fluid (as $\varepsilon\, We^2$ goes to zero) we arrive at the following expressions for Bejan number:

$$\begin{aligned} Be_T = {} & \left\{ Br\left(\frac{\Pi(\Pi-\beta)}{\Pi^2-1}\right)^2 \left(\frac{2}{R^3} + \frac{1-\Pi^2}{\Pi^2}\frac{1}{R\ln\Pi}\right) \right. \\ & \left. + \frac{1}{R\ln\Pi} \right\}^2 \\ & \times \left(\left\{ Br\left(\frac{\Pi(\Pi-\beta)}{\Pi^2-1}\right)^2 \left(\frac{2}{R^3} + \frac{1-\Pi^2}{\Pi^2}\frac{1}{R\ln\Pi}\right) \right. \right. \\ & \left. \left. + \frac{1}{R\ln\Pi} \right\}^2 + 4\frac{Br}{\Omega}\left(\frac{\Pi(\Pi-\beta)}{\Pi^2-1}\right)^2 \frac{1}{R^4} \right)^{-1} \end{aligned} \tag{34}$$

$$\begin{aligned} Be_q = {} & \left\{ 2\left(\frac{\Pi(\Pi-\beta)}{\Pi^2-1}\right)^2 \frac{Br}{R}\left(\frac{1}{R^2} - \frac{1}{\Pi^2}\right) + \frac{\Pi}{R} \right\}^2 \\ & \times \left(\left\{ 2\left(\frac{\Pi(\Pi-\beta)}{\Pi^2-1}\right)^2 \frac{Br}{R}\left(\frac{1}{R^2} - \frac{1}{\Pi^2}\right) + \frac{\Pi}{R} \right\}^2 \right. \\ & \left. + 4\frac{Br}{\Omega}\left(\frac{\Pi(\Pi-\beta)}{\Pi^2-1}\right)^2 \frac{1}{R^4} \right)^{-1} \end{aligned} \tag{35}$$

which again are not in agreement to those of Mahmud and Fraser [14] (compare Eqs. (17) and (18) of their work with Eqs. (34) and (35)).

3.6. Inner wall heat flux

In order to complete the solution, consider another thermal boundary condition in which, the inner cylinder is subjected to constant wall heat flux while the outer cylinder is kept at constant temperature

$$r = r_i \quad \Rightarrow \quad u_\theta = r_i\omega_i,\ -\frac{\partial T}{\partial r} = \frac{q}{k} \tag{2a}$$

$$r = r_o \quad \Rightarrow \quad u_\theta = r_o\omega_o,\ T = T_o \tag{3a}$$

If we adopt a similar procedure to that used for the previous boundary conditions (Eqs. (2) and (3)), we arrive at the following expressions for temperature profile, entropy generation number, and Bejan number

$$\begin{aligned} \Theta_q = {} & \frac{Br\,\tau_{wi}^{*2}}{36R^6\Pi^6(\Pi-1)^2}\left[9\Pi^4 R^4\left(R^2-\Pi^2\right) \right. \\ & \left. + 2\varepsilon\, We^2\, \tau_{wi}^{*2}\left(R^6 - \Pi^6\right)\right] \\ & + \left[-1 - \frac{Br\,\tau_{wi}^{*2}}{6(\Pi-1)^2}\left(3 + 2\varepsilon\, We^2\, \tau_{wi}^{*2}\right)\right]\ln\frac{R}{\Pi} \end{aligned} \tag{20a}$$

$$\begin{aligned} N_{Sq} = {} & \left\{ \frac{Br\,\tau_{wi}^{*2}}{6(\Pi-1)^2 R^7}\left(3R^4 + 2\varepsilon\, We^2\, \tau_{wi}^{*2}\right) \right. \\ & \left. + \left[-1 - \frac{Br\,\tau_{wi}^{*2}}{6(\Pi-1)^2}\left(3 + 2\varepsilon\, We^2\, \tau_{wi}^{*2}\right)\right]\frac{1}{R} \right\}^2 \\ & + \frac{Br\,\tau_{wi}^{*2}}{\Omega(\Pi-1)^2 R^8}\left(R^4 + 2\varepsilon\, We^2\, \tau_{wi}^{*2}\right) \end{aligned} \tag{28a}$$

$$\begin{aligned} Be_q = {} & \left\{ \frac{Br\,\tau_{wi}^{*2}}{6(\Pi-1)^2 R^7}\left(3R^4 + 2\varepsilon\, We^2\, \tau_{wi}^{*2}\right) \right. \\ & \left. + \left[-1 - \frac{Br\,\tau_{wi}^{*2}}{6(\Pi-1)^2}\left(3 + 2\varepsilon\, We^2\, \tau_{wi}^{*2}\right)\right]\frac{1}{R} \right\}^2 \\ & \times \left(\left\{ \frac{Br\,\tau_{wi}^{*2}}{6(\Pi-1)^2 R^7}\left(3R^4 + 2\varepsilon\, We^2\, \tau_{wi}^{*2}\right) \right. \right. \\ & \left. + \left[-1 - \frac{Br\,\tau_{wi}^{*2}}{6(\Pi-1)^2}\left(3 + 2\varepsilon\, We^2\, \tau_{wi}^{*2}\right)\right]\frac{1}{R} \right\}^2 \\ & \left. + \frac{Br\,\tau_{wi}^{*2}}{\Omega(\Pi-1)^2 R^8}\left(R^4 + 2\varepsilon\, We^2\, \tau_{wi}^{*2}\right) \right)^{-1} \end{aligned} \tag{33a}$$

In the above equations Θ is the dimensionless temperature and is defined as $(T - T_o)/\Delta T$.

4. Results and discussions

4.1. Flow and thermal fields

The flow field of PTT viscoelastic was discussed in details by Mirzazadeh et al. [22]. Therefore in this section we only focus on the heat transfer behavior of PTT fluid. Temperature profiles are presented in Fig. 2 for different values of Brinkman number ranges 0–6, in the case of isothermal boundary condition, and when the inner cylinder is rotating and the outer cylinder is at rest (i.e. $\beta = 0$). As it is apparent from this figure, the temperature profile exhibits a maximum value within the annular gap for $Br > 2$. This is because by increasing Brinkman number, the magnitude of viscous dissipation term increases in Eq. (4). The location of maximum temperature is also important, because at this position the entropy generation due to heat transfer is zero (i.e. $Be = 0$).

Fig. 3 shows the effect of fluid elasticity ($\varepsilon\, We^2$, ranges 0–100) on temperature profile for the case of inner cylinder rotation. As it can be seen from this figure, by increasing the fluid elasticity the value of maximum temperature decreases inside the annular space and for high Weissenberg number this maximum disappears. This behavior of fluid results from the shear thinning effect of PTT fluid, where the viscosity function and shear stress of fluid decreases with increasing fluid elasticity.

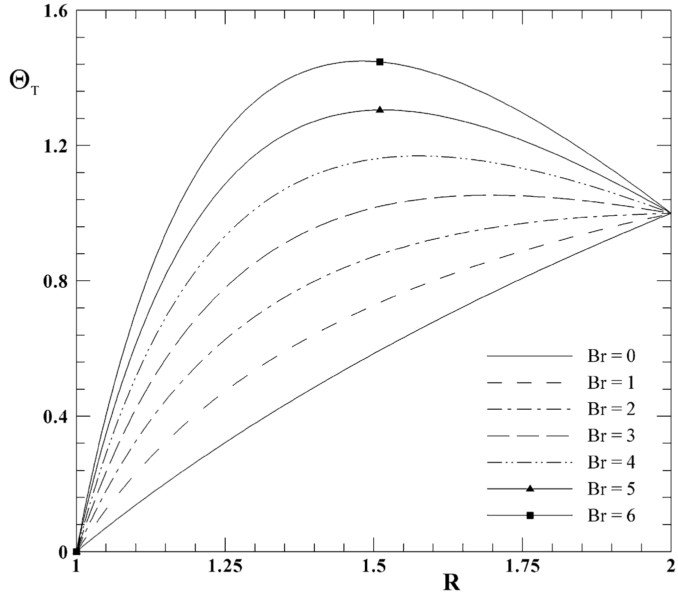

Fig. 2. Effect of Brinkman number on the temperature profile for isothermal boundary condition for $\Pi = 2$, $\beta = 0$, $\varepsilon\, We^2 = 0.1$.

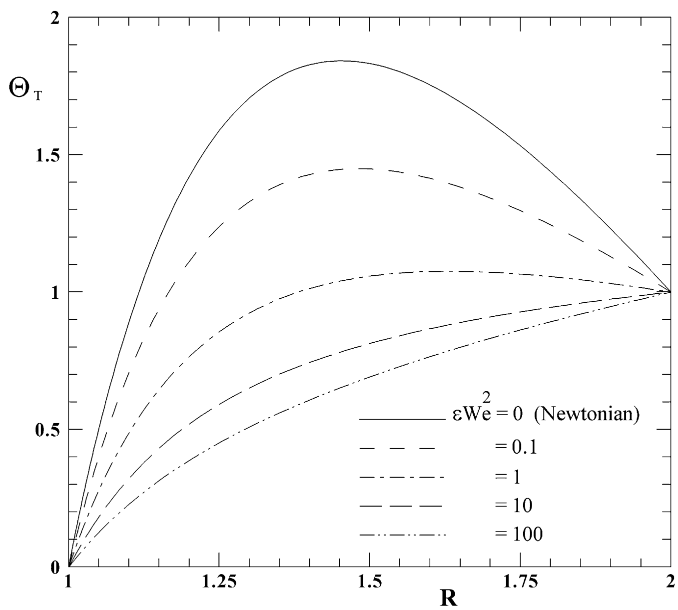

Fig. 3. Effect of fluid elasticity ($\varepsilon\, We^2$) on the temperature profile for isothermal boundary condition for $\Pi = 2$, $\beta = 0$, $Br = 6$.

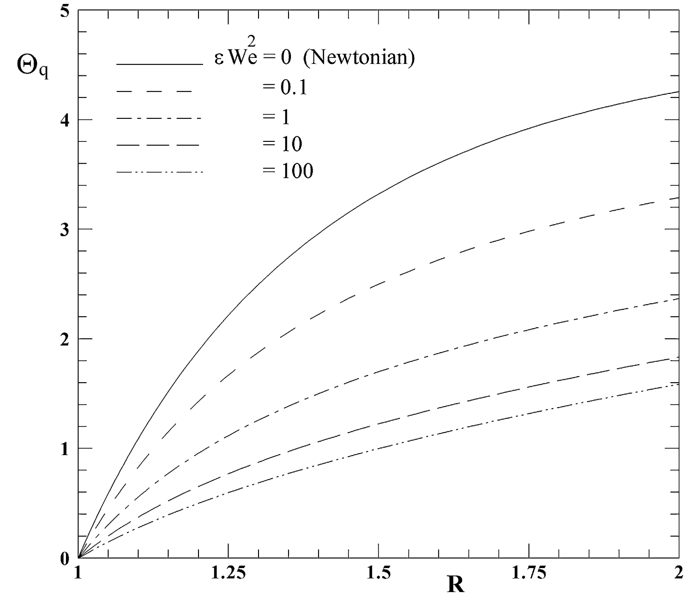

Fig. 4. Effect of fluid elasticity ($\varepsilon\, We^2$) on the temperature profile for isoflux boundary condition for $\Pi = 2$, $\beta = 0$, $Br = 4$.

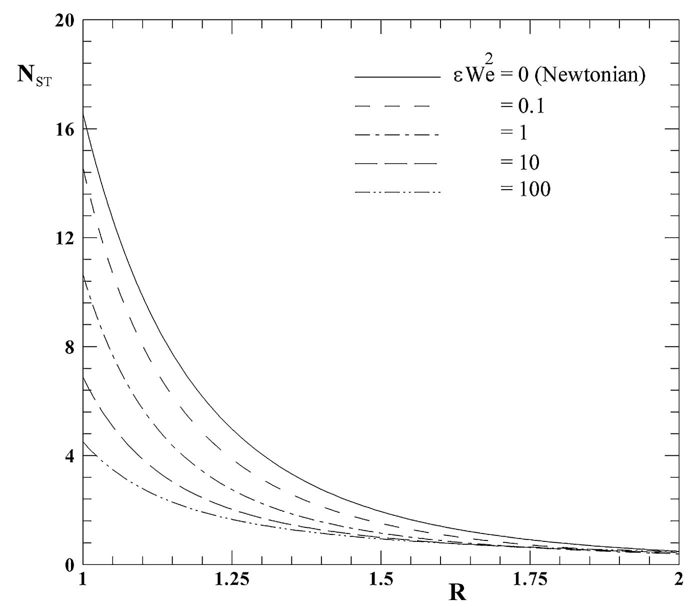

Fig. 5. Effect of fluid elasticity ($\varepsilon\, We^2$) on the isothermal entropy generation profiles for $\Pi = 2$, $Br = 1$, $Br/\Omega = 1$, $\beta = 0$.

A discussion of the viscosity function and the shear-thinning behaviour of a PTT fluid was given by Keunings and Crochet [27] and is discussed in greater detail by Pinho and Oliveira [28] (see e.g. Fig. 4 in their work). A similar remark can be made for the case of constant heat flux boundary condition (as is shown in Fig. 4), although the temperature profiles are not similar in shape to the isothermal case.

4.2. Local entropy generation

The influence of fluid elasticity ($\varepsilon\, We^2$, ranges 0–100) on dimensionless entropy generation numbers (N_{ST} and N_{Sq}) are shown in Figs. 5 and 6. The decrease in N_{ST} and N_{Sq} with increasing fluid elasticity is again attributable to the shear-thinning behaviour of the PTT fluid. it can be seen from these figures, as $\varepsilon\, We^2$ approaches zero the values of the N_{ST} and N_{Sq} are not in agreement with those for a Newtonian fluid (see Figs. 4 and 10 in Mahmud and Fraser [14] paper for $\Pi = 2$, $Br = 1$, β (λ in their work) $= 0$, $Br/\Omega = 1$), which is again related to the mistake made in the derivation of the equations of their work.

Bejan number (Be) is another important parameter which is usually used in analyzing entropy generation problems, and based on definition (Eq. (31)), the value of Bejan number in-

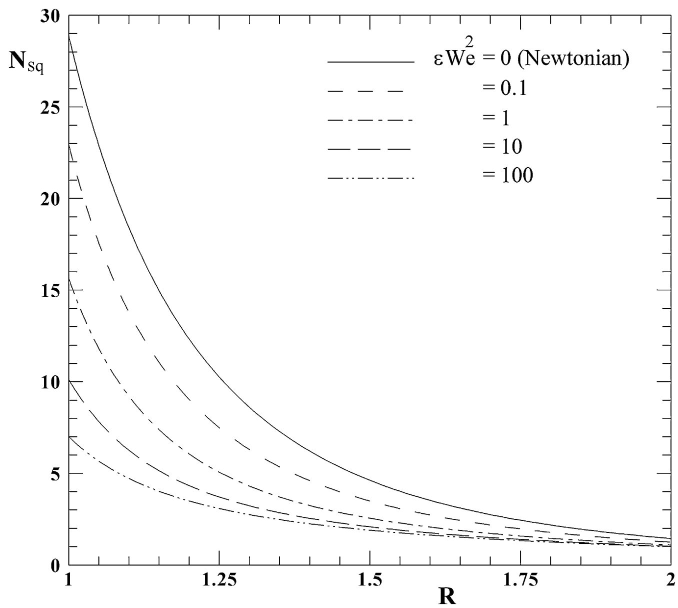

Fig. 6. Effect of fluid elasticity ($\varepsilon\, We^2$) on the isoflux entropy generation profiles for $\Pi = 2$, $Br = 1$, $Br/\Omega = 1$, $\beta = 0$.

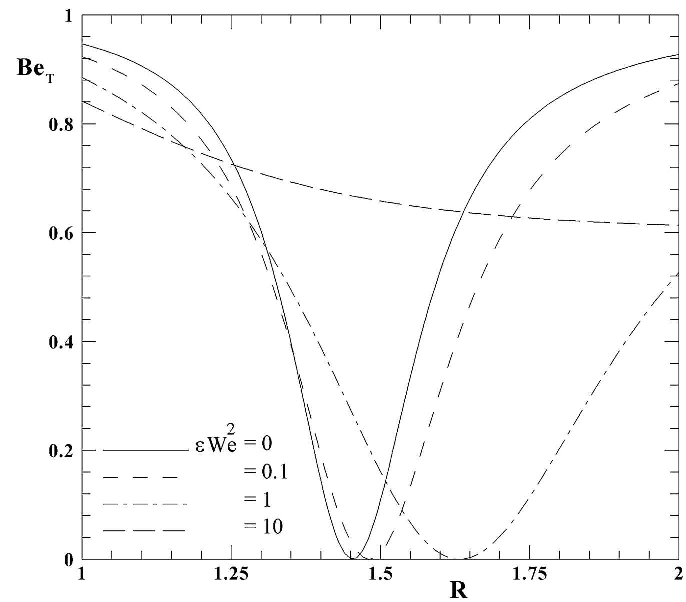

Fig. 8. Effect of fluid elasticity ($\varepsilon\, We^2$) on the isothermal Bejan number profiles for $\Pi = 2$, $Br = 6$, $Br/\Omega = 1$, $\beta = 0$.

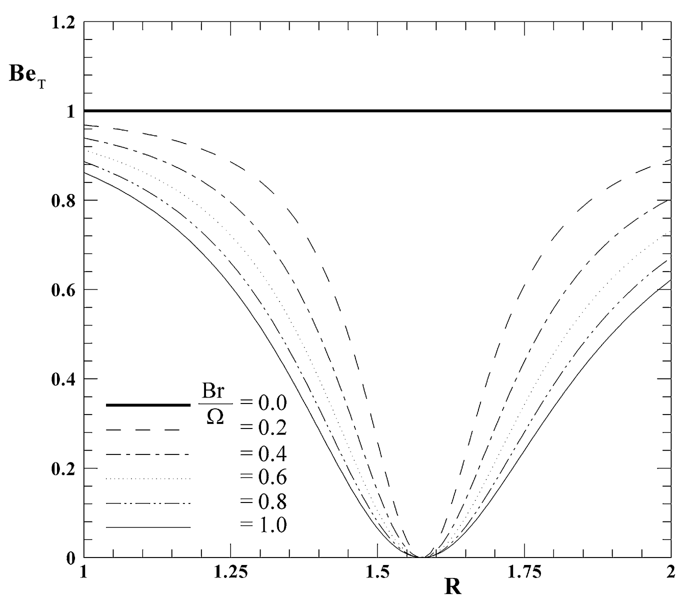

Fig. 7. Isothermal Bejan number profiles at different group parameters (Br/Ω) for $\Pi = 2$, $\beta = 0$, $Br = 4$, $\varepsilon\, We^2 = 0.1$.

dicates whether the entropy generation is dominated by heat transfer or fluid friction. Fig. 7 represents the effect of group parameter (Br/Ω, ranges 0–1) on Bejan number (Be_T) for $\Pi = 2$, $Br = 4$, $\beta = 0$, $\varepsilon\, We^2 = 0.1$. As it is shown in this figure for $Br/\Omega = 0$ the Bejan number is equal to 1 which means there is no fluid friction contribution to entropy generation. However, as Br/Ω increases the Bejan number decreases which means the fluid friction contribution to entropy generation increases. Another important finding from this figure is that for all values of the group parameters ($Br/\Omega > 0$), the Bejan number profile exhibits a minimum value within the annular gap which is due to the occurrence of the maximum in the temperature profile. The radial location of minimum Bejan number is independent of the values of group parameters and this location is the same as the radial location of maximum temperature ($R_{\min} \approx 1.58$). The value of minimum Bejan number for all values of group parameters is zero. This is because the occurrence of maximum in temperature profile implies the zero temperature gradient ($\partial\Theta/\partial R = 0$) and consequently Bejan number becomes zero with respect to its definition (see Eqs. (31) and (26)). The zero value of Bejan number indicates that, there is no heat transfer contribution to the entropy generation or in other words, the entropy generation is dominated only by fluid friction.

The effect of fluid elasticity ($\varepsilon\, We^2$, ranges 0–10) on the radial distribution of Bejan number is shown in Fig. 8. As it can be seen from this figure, for lower values of fluid elasticity ($\varepsilon\, We^2 \leqslant 1$) the Bejan number falls rapidly along the radial direction and touches the minimum value (=0) and then increases toward the outer cylinder. The radial location of minimum Bejan number shifts toward the outer cylinder and its value is same as the radial location of maximum point in the temperature profile (see Fig. 3). For higher values of fluid elasticity ($\varepsilon\, We^2 > 1$) the Bejan number profile doesn't show any minimum within the annular gap, which is due to the absence of maximum point in the temperature profile (see e.g. Fig. 3).

4.3. Global entropy generation

The dimensionless volumetric average entropy generation rate ($[N_S]_{\mathrm{av}}$) can be evaluated as below:

$$[N_S]_{\mathrm{av}} = \frac{1}{\forall}\int_{\forall} N_S \,\mathrm{d}\forall = \frac{1}{\forall}\int_{\forall} N_S r \,\mathrm{d}\theta\,\mathrm{d}r\,\mathrm{d}z \tag{36}$$

For the case of isothermal boundary condition, the average entropy generation rate ($[N_{ST}]_{\mathrm{av}}$) can be obtained by substitution Eq. (27) into Eq. (36)

$$[N_{ST}]_{av} = \frac{2}{\Pi^2 - 1}\left(C^2 \operatorname{Ln}\Pi + \sum_{n=0}^{6} \frac{A_n}{\Pi^{2n}}\right) \tag{37}$$

where

$$A_o = \frac{1}{12}\left(B^2 + 3A^2 + 6E + 2F + 12AC + 4BC + 3AB\right)$$
$$A_1 = -\frac{2AC + E}{2}, \qquad A_2 = -\frac{A^2}{4}, \qquad A_3 = -\frac{2BC + F}{6}$$
$$A_4 = -\frac{AB}{4}, \qquad A_5 = 0, \qquad A_6 = -\frac{B^2}{12} \tag{38}$$

constants A, B, C, E, and F are defined as below:

$$A = \frac{Br\,\tau_{wi}^{*2}}{2(\Pi - 1)^2}, \qquad B = \frac{Br\,\tau_{wi}^{*4}\varepsilon\,We^2}{3(\Pi - 1)^2}$$
$$C = \left[1 + \frac{Br\,\tau_{wi}^{*2}}{36(\Pi - 1)^2\Pi^6}\left(9\Pi^4\left(1 - \Pi^2\right) + 2\varepsilon\,We^2\tau_{wi}^{*2}\left(1 - \Pi^6\right)\right)\right] / \ln\Pi$$
$$E = \frac{Br}{\Omega}\frac{\tau_{wi}^{*2}}{(\Pi - 1)^2}, \qquad F = 2\frac{Br}{\Omega}\frac{\tau_{wi}^{*4}\varepsilon\,We^2}{(\Pi - 1)^2} \tag{39}$$

As it can be seen from the above equations, the average entropy generation rate ($[N_{ST}]_{av}$) is a function of geometric parameter Π, velocity ratio β, fluid elasticity $\varepsilon\,We^2$, Brinkman number Br, and group parameter Br/Ω. Fig. 9 shows the effect of group parameter (Br/Ω, ranges 0–4) on average entropy generation rate ($[N_{ST}]_{av}$) for $\Pi = 2$, $\varepsilon\,We^2 = 0.1$, and $Br = 1$. As it can be seen from this figure, average entropy generation rate ($[N_{ST}]_{av}$) increases by increasing group parameter (Br/Ω). $[N_{ST}]_{av}$ profile shows a minimum at $\beta = 2$, where the magnitude of this minimum ($[N_{ST}]_{av,min} \approx 0.9618$) is same for all values of group parameters. An important finding from Fig. 9 is that, the location of minimum average entropy generation rate

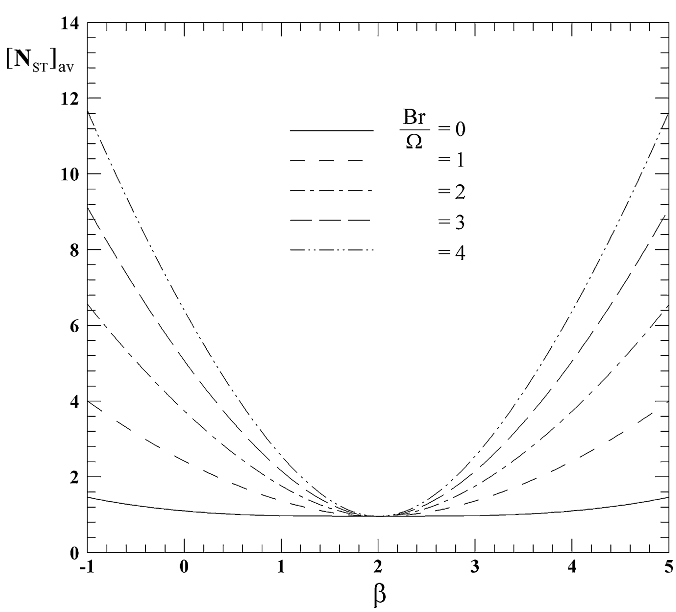

Fig. 9. Average entropy generation profiles at different group parameters (Br/Ω) for isothermal boundary condition for $\Pi = 2$, $Br = 1$, $\varepsilon\,We^2 = 0.1$.

and also the magnitude of this point ($[N_{ST}]_{av,min}$) are independent of the values of Brinkman number and group parameter. In both of these figures, the location of minimum average entropy generation rate happen at $\beta = \Pi = 2$ and therefore this velocity ratio leads to a condition at which the angular velocity of inner cylinder (ω_i) is same as the angular velocity of outer cylinder (ω_o) (i.e. there is no relative angular motion between cylinders). At this condition the shear stress between fluid layers will be zero ($\tau_{r\theta} = 0$ or $\tau_{wi}^* = 0$) and hence the fluid contribution to entropy generation will be zero (see Eqs. (26) and (27)). A similar result was obtained previously by Mahmud and Fraser [14] for the annular flow of Newtonian fluid: they concluded that $\beta = \Pi$ is the location of minimum average entropy generation rate and also this location is independent of the values of Brinkman number and group parameter. Substitution $\tau_{wi}^* = 0$ in Eqs. (39), (38), and (37) results in the following equation for $[N_{ST}]_{av,min}$:

$$[N_{ST}]_{av,min} = \frac{2}{(\Pi^2 - 1)\operatorname{Ln}\Pi} \tag{40}$$

Eq. (40) indicates that the value of $[N_{ST}]_{av,min}$ is only a function of Π and is independent of Br, Br/Ω, and $\varepsilon\,We^2$. A similar conclusion can be reached for the case of isoflux boundary condition. In other words the average entropy generation rate again shows a minimum at $\beta = \Pi$. Performing a similar procedure to that of isothermal boundary condition results in the following equation for minimum average entropy generation rate ($[N_{Sq}]_{av,min}$) in the case of isoflux boundary condition

$$[N_{Sq}]_{av,min} = \frac{2\Pi^2 \operatorname{Ln}\Pi}{\Pi^2 - 1} \tag{41}$$

The minimum value of average entropy generation rate is only a function of geometric parameter (Π). Therefore, the effect of this parameter (Π, ranges 0–5) on the minimum value of average entropy generation rate for both cases of isothermal and isoflux boundary conditions are shown in Fig. 10. As it can be seen from this figure at $\Pi = 1.763$ the value of minimum entropy generation ($[N_S]_{av,min} = 1.672$) are equal for both boundary conditions.

The influence of fluid elasticity ($\varepsilon\,We^2$, ranges 0–10) on the average entropy generation rate ($[N_{ST}]_{av}$) is shown in Fig. 11. As it can be seen, by increasing fluid elasticity, average entropy generation rate ($[N_{ST}]_{av}$) decreases. This is again related to the shear thinning behavior of PTT viscoelastic fluids, where the magnitudes of viscosity, shear stress, and temperature gradients decrease by increasing fluid elasticity, and consequently results in a decrease in the magnitude of average entropy generation rate. An important finding from this figure is that, in comparison with Newtonian fluids, more than 40% decrease in the magnitude of average entropy generation rate can be achieved when $\varepsilon\,We^2$ approaches 1 (for $\Pi = 2$).

4.4. Wall cooling condition

According to the definition of wall heat flux adopted in this work (see Eq. (3)), a positive value of wall heat flux ($q > 0$)

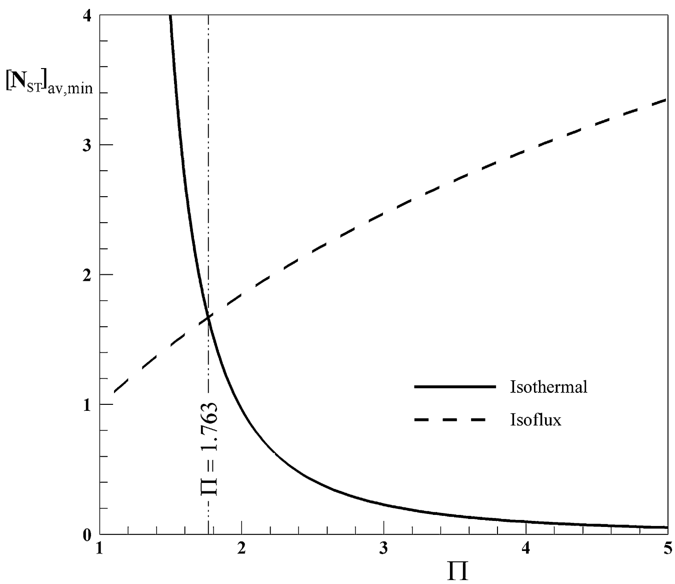

Fig. 10. Minimum average entropy generation profiles for isothermal and isoflux boundary conditions.

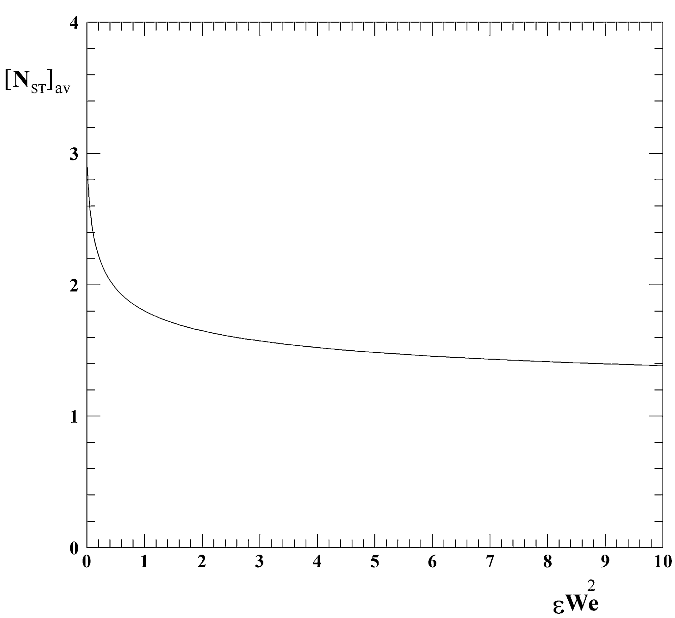

Fig. 11. Average entropy generation rate vs fluid elasticity ($\varepsilon\, We^2$) for isothermal boundary condition for $\Pi = 2$, $Br = 1$, $Br/\Omega = 1$, $\beta = 0$.

implies that heat is being supplied across the wall into the fluid and definition of Brinkman number requires that $Br > 0$, while, a negative value of wall heat flux ($q < 0$) implies that heat is being removed from the outer wall and consequently requires that $Br < 0$. Even though, the present solution is valid for both cases of wall heating and wall cooling but the trend of results are different. For example, the influence of Brinkman number (Br, ranges from −6 to 4) on the average entropy generation rate ($[N_{Sq}]_{av}$) is shown in Fig. 12. As it can be seen from this figure for low absolute values of Br, a negative wall heat flux overcomes the effect of viscous dissipation and then results in a decrease in the average entropy generation rate; however, if Br exceeds a certain limiting value, the heat generated internally

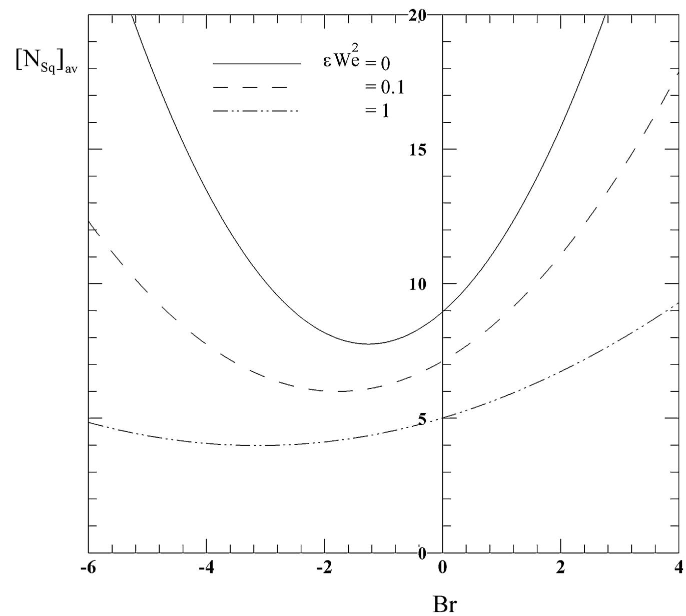

Fig. 12. Effect of Brinkman number (wall cooling and wall heating) on average entropy generation rate for different values of fluid elasticity ($\varepsilon\, We^2$) for $\Pi = 2$, $Br/\Omega = 4$, $\beta = 0$.

by viscous processes will overcome the effect of wall cooling and therefore the average entropy generation rate increases. Another important finding from this figure is that, increasing the magnitude of fluid elasticity, increases the range of Brinkman number over which the effect of wall cooling overcomes the effect of viscous dissipation. This is because by increasing the fluid elasticity the heat generated internally by viscous dissipation decreases due to the shear thinning behavior of the fluid.

5. Conclusions

In this study, forced convection heat transfer and entropy generation analysis were investigated for purely tangential flow of nonlinear viscoelastic fluid obeying the simplified form of Phan-Thien–Tanner (SPTT) constitutive equation between concentric annulus where the inner and outer cylinders are rotating with different angular velocities. Two different types of boundary conditions are examined: at the first case both cylinders are isothermal and kept at different temperatures and in the second case the heat flux is kept constant at the outer cylinder and the inner is isothermal. Analytical expressions for temperature profile, entropy generation number, and the Bejan number are derived. The effect of velocity ratio (β), the group parameter (Br/Ω), the Brinkman number (Br), and fluid elasticity ($\varepsilon\, We^2$) on the above parameters were investigated. The conclusions of the present study can be summarized as below:

1. For the case of isothermal boundary condition and for higher values of Brinkman number, the temperature profile exhibits a maximum within the annular gap, where the magnitude of this maximum decreases by increasing the fluid elasticity which is due to the shear thinning behavior of PTT fluid.

2. The entropy generation number increases by increasing group parameter (Br/Ω).
3. The entropy generation number for both cases of isothermal and isoflux boundary conditions decreases with increasing fluid elasticity which is again attributable to the shear-thinning behaviour of the PTT fluid.
4. Contribution of the fluid friction to entropy generation increases (i.e. Bejan number decreases) by increasing Br/Ω.
5. All Bejan number profiles show a minimum inside the annular gap until the temperature profiles exhibit a maximum temperature. The radial location of minimum Bejan number is exactly the same as the radial location of maximum temperature. The magnitude of minimum Bejan number is zero ($Be_{\min} = 0$).
6. The maximum value of Bejan number (i.e. maximum heat transfer irreversibility) occurs at the inner cylinder where the velocity and temperature gradients are maximum.
7. Although the average entropy generation rate ($[N_{ST}]_{\text{av}}$) is a function of geometric parameter (Π), group parameter (Br/Ω), Brinkman number (Br), velocity ratio (β), and fluid elasticity ($\varepsilon\, We^2$), However, the location of minimum average entropy generation rate is only a function of geometric parameter (Π) and always this minimum occurs at $\beta = \Pi$ (condition at which the angular velocity of inner and outer cylinders are equal, i.e. there is no relative rotation).
8. Average entropy generation rate ($[N_{ST}]_{\text{av}}$) increases as group parameter (Br/Ω) and Brinkman number increase.
9. Finally, the average entropy generation rate ($[N_{ST}]_{\text{av}}$) decreases by increasing fluid elasticity ($\varepsilon\, We^2$) which is due to the shear-thinning behavior of PTT fluid. In fact, more than 40% decrease in the magnitude of average entropy generation rate can be achieved when $\varepsilon\, We^2$ approaches 1 (for $\Pi = 2$).

References

[1] D.M. Maron, S. Cohen, Hydrodynamics and heat/mass transfer near rotating surfaces, Adv. Heat Transfer 21 (1991) 141–183.

[2] P.R.N. Childs, C.A. Long, Review of forced convective heat transfer in stationary and rotating annuli, Proc. IMechE C: Mech. Eng. Sci. 210 (1996) 123–134.

[3] M.P. Escudier, P.J. Oliveira, F.T. Pinho, Fully developed laminar flow of purely viscous non-Newtonian liquids through annuli including the effects of eccentricity and inner cylinder rotation, Int. J. Heat Fluid Flow 23 (1) (2002) 52–73.

[4] K. Khellaf, G. Lauriat, Numerical study of heat transfer in a non-Newtonian Carreau-fluid between rotating concentric vertical cylinders, J. Non-Newtonian Fluid Mech. 89 (2000) 45–61.

[5] M. Naimi, R. Devienne, M. Lebouché, Etude dynamique et thermique de l'écoulement de Couette–Taylor–Poiseuille ; cas d'un fluide présentant un seuil d'écoulement (Dynamical and thermal study of Couette–Taylor–Poiseuille flow; case of yield pseudo-plastic fluid), Int. J. Heat Mass Transfer 33 (1990) 381–391.

[6] R.M. Manglik, P. Fang, Thermal processing of viscous non-Newtonian fluids in annular ducts: effects of power-law rheology, duct eccentricity, and thermal boundary conditions, Int. J. Heat Mass Transfer 45 (2002) 803–814.

[7] M. Capobianchi, T.F. Irvine Jr., Predictions of pressure drop and heat transfer in concentric annular ducts with modified power-law fluids, Wärme Stofübertragung 27 (1992) 209–215.

[8] A. Bejan, Second-law analysis in heat transfer and thermal design, Adv. Heat Transfer 15 (1982) 1–58.

[9] A. Bejan, A study of entropy generation in fundamental convective heat transfer, J. Heat Transfer 101 (1979) 718–725.

[10] P.K. Nag, N. Kumar, Second law optimization of convective heat transfer through a duct with constant heat flux, Int. J. Energy Res. 13 (1989) 537–543.

[11] A.Z. Sahin, Second law analysis of laminar viscous flow through a duct subjected to constant wall temperature, J. Heat Transfer 120 (1998) 76–83.

[12] A.Z. Sahin, Effect of variable viscosity on the entropy generation and pumping power in a laminar fluid flow through a duct subjected to constant heat flux, Heat Mass Transfer 35 (1999) 499–506.

[13] B.S. Yilbas, Entropy analysis of concentric annuli with rotating outer cylinder, Exergy Int. J. 1 (2001) 60–66.

[14] S. Mahmud, R.A. Fraser, Analysis of entropy generation inside cylindrical annuli with relative rotation, Int. J. Thermal Sci. 42 (2003) 513–521.

[15] O.M. Haddad, M.K. Alkam, M.T. Khasawneh, Entropy generation due to laminar forced convection in the entrance region of a concentric annulus, Energy 29 (2004) 35–55.

[16] S. Mahmud, R.A. Fraser, Second law analysis of forced convection in a circular duct for non-Newtonian fluids, Energy 31 (2006) 2226–2244.

[17] M. Pakdemirli, B.S. Yilbas, Entropy generation for pipe flow of a third grade fluid with Vogel model viscosity, Int. J. Non-Linear Mech. 41 (2006) 432–437.

[18] N. Phan-Thien, R.T. Tanner, A new constitutive equation derived from network theory, J. Non-Newtonian Fluid Mech. 2 (1977) 353–365.

[19] N. Phan-Thien, A non-linear network viscoelastic model, J. Rheology 22 (1978) 259–283.

[20] P.J. Oliveira, F.T. Pinho, Analytical solution for fully developed channel and pipe flow of Phan-Thien–Tanner fluids, J. Fluid Mech. 387 (1999) 271–280.

[21] D.O.A. Cruz, F.T. Pinho, Skewed Poiseuille–Couette flow of SPTT fluids in concentric annuli and channels, J. Non-Newtonian Fluid Mech. 121 (2004) 1–14.

[22] M. Mirzazadeh, M.P. Escudier, F. Rashidi, S.H. Hashemabadi, Purely tangential flow of a PTT-viscoelastic fluid within a concentric annulus, J. Non-Newtonian Fluid Mech. 129 (2005) 88–97.

[23] R.I. Tanner, Engineering Rheology, Clarendon Press, Oxford, 2000.

[24] R.B. Bird, R.C. Armstrong, O. Hassager, Dynamics of Polymeric Liquids, Fluid Mechanics, vol. I, second ed., Wiley, 1987.

[25] A. Bejan, Entropy Generation Minimization, CRC, Boca Raton, NY, 1996.

[26] S. Paoletti, F. Rispoli, E. Sciubba, Calculation of exergetic losses in compact heat exchanger passages, ASME AES 10 (1989) 21–29.

[27] R. Keunings, M.J. Crochet, Numerical simulation of the flow of a viscoelastic fluid through an abrupt contraction, J. Non-Newtonian Fluid Mech. 14 (1984) 279–299.

[28] F.T. Pinho, P.J. Oliveira, Axial annular flow of non-linear viscoelastic fluid-an analytical solution, J. Non-Newtonian Fluid Mech. 93 (2000) 325–337.